韓國鑛物學會誌 第3卷 第2號 (1990)
J. Miner. Soc. Korea, 3, 79-88 (1990)

Iron Oxide Minerals in the Sancheong Kaolin Deposits

산청지역 고령토 광상에서 산출되는 산화철 광물

Gi-Young Jeong (정 기 영) and Soo Jin Kim (김 수 진)
Department of Geological Sciences, Seoul National University, Seoul 151-742, Korea
(서울대학교 자연과학대학 지질과학과)

ABSTRACT : The occurrence and textural relations of iron oxide minerals in kaolin suggest that they are derived mainly from amphibole and chlorite in precursor anorthositic rocks. X-ray diffraction analyses show that yellow color is due to goethite and reddish brown color to the coexistence of hematite and goethite. Goethite is dominant in the lower white kaolin where chlorite alters to vermiculite and amphibole dissolves, whereas hematite occurs together with goethite in the upper reddish brown kaolin and fissure where amphibole, vermiculite, and chlorite are subjected to intensive leaching. The Al substitution for Fe ranges from 6 to 26 mol% in goethite and from 5 to 8 mol% in hematite. There is a linear relation between goethite and hematite in Al substitution. Mean crystallite dimensions calculated from diffraction line broadness of goethite and hematite are below 340 A. Goethite is slightly acicular, whereas hematite is tabular. Electron microscopy shows that goethite associated with vermiculite is commonly acicular or star-shaped but less acicular in the upper reddish brown kaolin. Hematite shows hexagonal or spherical shape but more irregular shape in the upper reddish brown kaolin. Goethite and hematite in the upper reddish brown kaolin are poorly crystalline. The mineralogy of hematite and goethite is compared with other synthetic ones, and discussed in the genetic aspect. It is suggested that the climatic factors for the formation of two iron oxides overlap in this area.

요약 : 고령토의 조직과 산출상태의 관찰결과 산화철 광물을 침전시킨 철의 주요 근원은 모암인 회장암에 함유된 각섬석과 녹니석이다. X선 회절 분석결과 침철석은 녹니석이 버미큘라이트로 변질되고 각섬석이 용해되기 시작하는 하부 백색 광석에서 우세하며, 적철석은 각섬석, 녹니석 및 버미큘라이트가 심한 용탈작용을 받는 상부 적갈색 광석이나 열개에서 침철석과 함께 산출된다. 침철석 및 적철석내 Fe에 대한 Al의 치환량은 각각 6~26 mol% 및 5~8 mol%이며 이 두 값 사이에는 비례 관계가 있다. 회절선폭의 크기로부터 계산된 침철석과 적철석의 평균 입자크기는 340Å 이하이며 침철석은 약간의 침상을 보이는 반면 적철석은 탁상이다. 전자현미경 관찰에 의하면 버미큘라이트와 수반되는 침철석은 침상 또는 성상이나 적갈색 광석에서는 그러한 특징이 작다. 적철석은 육각 또는 원형을 보이나 상부 적갈색 광석에서는 보다 불규칙한 모양이다. 적철석과 침철석의 광물학적 특성을 합성실험에서 보고된 결과들과 비교하여 성인적 측면에서 논의되었다. 이 지역에서는 침철석과 적철석의 생성에 적합한 기후조건들이 중첩된 것으로 생각된다.

INTRODUCTION

Kaolins in the Hadong-Sancheong area are often stained with yellowish, yellowish brown, red, reddish brown, and pink tint depending on their mineral composition and weathering degree (Jeong, 1987; Kim et al., 1988). Kaolin in the lower zone of the deposit shows, in general, white or pale pink color. It usually has yellow or yellowish brown spots and bands which are the relic textures of parent anorthositic rocks. The spots and bands consist mainly of decomposed product

of amphibole and chlorite. Kaolin in the upper zone shows pink, red, and reddish brown color. It still preserves most original textures of parent rock except in the uppermost part. The kaolin deposits are in general covered with 1-2 m thick soil layer where the textures of parent rock are completely destroyed showing deep reddish brown color due to the high content of iron oxides and organics. Excluding the amphibole residue and vermiculite, the colors of the kaolin and soil are originated from the microcrystalline iron oxide precipitates.

The iron oxide minerals formed in the weathering profile are commonly microcrystalline to pooly-crystalline, so that their identification is very difficult. Microcrystalline iron oxide minerals in the weathering profile were extensively studied by soil scientists to explain the colors of soils and resolve pedogenesis (Schwertmann, 1988a; Schwertmann and Taylor, 1977) and so, precise identification methods and genetic relations between the iron oxide species have been established.

The present study was designed 1) to investigate the occurrence of iron oxides in the kaolin, 2) to characterize the iron oxides applying various techniques, and 3) to discuss their genesis.

EXPERIMENTAL METHODS

Colored kaolin samples were collected from the profile of the kaolin deposits according to their occurrence and color. 300 g of each kaolin sample was slightly crushed in a porcelain mortar and dispersed in distilled water with ultrasonic agitation for 5 minutes. The suspended fraction was transferred to a 2-liter settling cylinder. PH was adjusted to 10 with 1N NaOH solution to avoid flocculation. After overnight sedimentation, the suspended fraction was centri-fuged to separate clay.

Chemical treatments were carried out to selectively extract iron oxides from the prepared kaolin samples. Boiling 5M NaOH mehtod of Norrish and Taylor's(1961) was used to dissolve halloysite and kaolinite, and to concentrate iron oxides. In this method, 100 mℓ of 5M NaOH was added to a 1g sample in a 100 mℓ teflon beaker and covered with glass dish. After 1 hour boiling on a sand bath, the residue was separated by centrifuge after cooling, and subsequently treated with 0.5N HCl to dissolve sodalite which was formed during the treatment. After two times washing with ethanol, iron oxide concentrate was oven-dried at 60℃. Dithionite-citrate-bicarbonate (DCB) method was used to selectively extract iron oxides according to Mehra and Jackson(1960). 20 mℓ of 0.3 M Na-citrate, 0.5 g of $Na_2S_2O_4$, and 2.5 mℓ of 1M $NaHCO_3$ were mixed with a 0.5 g sample in a 50 mℓ centrifuge tube and shaked at 80℃ for 15 minutes. The extraction was repeated three times. Acid-oxalate extraction was carried out according to Schwertmann (1959). The raw and concentrate were decomposed with HF-HCl-HNO_3 to measure iron contents by atomic absorption spectrometry. Instrumentation Laboratory model IL 251 spectrophotometer was used with air-acetylene flame.

X-ray diffraction patterns of raws and concentrates were obtained in 9°−90° (2θ) range using Rigaku RAD3-C horizontal goniometer X-ray diffractometer with Co Kα radiation. Sample was packed in 10 mm×20 mm×0.2 mm size cavity of glass holder. Slit size and scanning speed were 1°−0.15 mm−1° and 2°/min, respectively. Diffraction line positions were accurately measured using $Pb(NO_3)_2$ powder as an internal standard.

Al-substitution of goethite was determined by the regression line AlOOH mol%=1730−572c_o (Å) which was obtained from the synthesis experiment of Schulze (1984). The c_o-dimension of the goethite unit cell was calculated from the d-values of (110) and (111) lines. Al-substitution of hematite was determined from the a_o-dimension of the hematite unit cell which was calculated from the d-value of (300) line. The regression line Al_2O_3 mol %=2932−582a_o was obtained from Schwertmann et al. (1979)'s Fig. 2.

Mean crystallite dimension was calculated from the Scherrer's equation(Klug and Alexander, 1974; Brindley, 1980). Half height peak width was corrected by instrumental broadening measured with quartz.

For sample B29, differential X-ray diffraction was attempted to confirm the presence of

ferrihydrite(Schulze, 1981). For this work, the sample was step-scanned in 20°~90°(2θ) range by counting for 10 sec per 0.02° step. Acid-oxalate treated sample's intensity data were subtracted from the untreated sample's intensity data after multiplication with optimum scale factor.

Differential thermal analysis of goethite was run on 30mg samples using Shimadzu DT20B instrument operated at a heating rate of 10℃/min with α-Al_2O_3 as an inert material.

Transmission electron micrographs were obtained using JEOL JEM 200CX electron microscope operated at 160 KV. The iron oxide samples were dispersed in methanol by ultrasonic agitation and loaded on the carbon-coated collodion copper grit of 3mm-diameter.

RESULTS AND DISCUSSION

Release of Iron from Amphibole and Chlorite

The precursors of the kaolin in the study area are anorthositic rocks which consist mainly of plagioclase (labradorite to bytownite in composition) with minor amphibole, chlorite, biotite, muscovite, epidote, and ilmenite (Jeong, 1980; Jeong, 1987; Kim et al. 1989). In author's recent microprobe works, the layer silicate mineral described as biotite in the previous work was identified to chlorite which is optically similar to biotite. Therefore, amphibole and chlorite are the main iron-bearing minerals in the anorthositic rocks. The microprobe analyses (not given here) show that amphibole corresponds compositionally to hornblende according to the nomenclature of Leake(1978), and chlorite corresponds to magnesian chamosite or ferroan chlinochlore according to AIPEA nomenclature (Baily, 1980).

From above results, it is concluded that the iron for the formation of the iron oxides has been released from amphibole and chlorite in the kaolinization process of the anorthositic rocks under supergene weathering environment.

The kaolin preserves the original textures of anorthositic rocks such as mafic bands and spots. In the lower white kaolin zone, the relic bands and spots show yellowish brown or green color. These bands and spots consist of altered products of amphibole and chlorite. In this early stage of alteration, hornblende begins to dissolve but still preserves the most original shape of the grain and thus the bands and spots still appear to be green in color, but iron oxides are often precipitated giving yellowish brown color around them. Chlorite is completely transformed to yellowish brown vermiculite which is also partially altered to kaolinite. The iron released during the transformation from chlorite to vermiculite has been precipitated as iron oxides in and around the bands and spots. DCB treatment of vermiculite flakes converts its yellowish brown color to green, implying that the yellowish brown color is due to iron oxide precipitate. This iron oxide has been identified as goethite by the 4.18Å X-ray diffraction line.

The kaolin in the upper part of the profile is stained with yellowish brown, reddish brown, red, and pink. The amphibole grain dissolves at a higher rate under intensive leaching condition, releasing high amount of iron which precipitates to reddish brown iron oxides. Vermiculite is altered to kaolinite, releasing iron for the precipitation of iron oxides.

The reddish brown vertical veinlets where iron oxide content is relatively higher than the other parts, are often observed in the upper part of the profile.

Highly leaching condition in this area is reflected in the presence of limonite layer 4cm thick in the upper part of the weathering profile which has been formed on the hornblende gneiss. The limonite layer looks like a thin continuous dark brown bed that consists mostly of goethite. It is developed in parallel to the foliation of gneiss at 2m below from the surface.

Mineralogy of Iron Oxides

X-ray diffraction analyses: Representative X-ray diffraction pattern of goethite and hematite concentrate is given in Fig. 1. It has been reported that Fe^{3+} in the structure of goethite and hematite can be substituted partially by Al^{3+} (Norrish and Taylor, 1961; Schwertmann et al., 1979). The Al contents in goethite and hematite calculated from the X-ray line shift are given in Table 1.

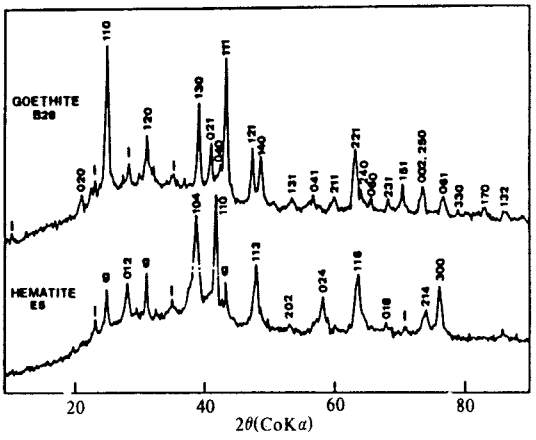

Fig. 1. X-ray diffraction pattern of goethite and hematite concentrated by 5M NaOH method (i: illite, g: goethite).

The AlOOH contents of goethite in the kaolin range from 6 to 26 mol %. It is known from both the synthesis study (Thiel, 1963; Schulze, 1984) and the investigation of natural samples (Schwertmann, 1988b) that Al substitutes for Fe in goethite up to 33 mol%. Except two yellowish brown samples (A12-2, and B25-2), the high Al substitution ranging from 15 to 26 mol % in goethite is similar to those of highly weathered soils of subtropical to tropical areas(Schwertmann, 1988b).

The Al_2O_3 contents of hematite range from 5 to 8 mol %. It is reported that Al in hematite substitutes for Fe up to 16 mol % (Caillière et al., 1960; Schwertmann et al., 1979). There exists a linear relationship in the Al substitution between goethite and hematite in the same kaolin sample (Fig. 2).

The X-ray diffraction profiles in Fig. 2 show that individual line is broadened variously. The broadness of the (hkl) lines can be used to calculate the dimension of a coherent X-ray

Table 1. Calculated Al contents of goethite and hematite.

Sample	C13-3	B29	G6	C17	E5	D2-2	B25-2	A12-2	B28
AlOOH mol% in goethite	15.7	26.1	21.1	21.7	23.5	18.5	6.4	9.0	20.9
Al_2O_3mol% in hematite	5.0	7.6	6.1	7.6	6.4	5.5			

* Calculation was not carried out for B19 due to its low peak intensity.

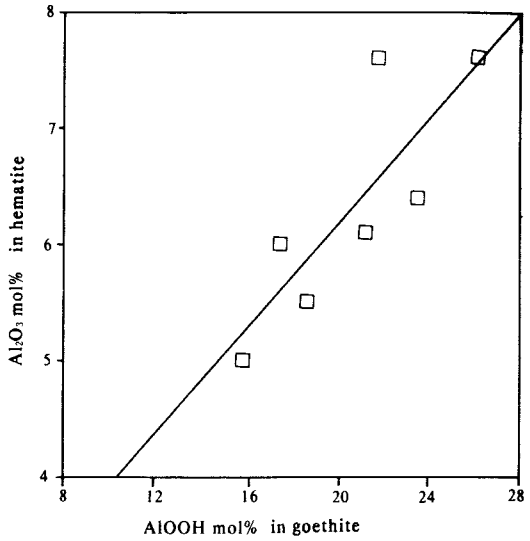

Fig. 2. Linear relation between the AlOOH mol % of goethite and the Al_2O_3mol % of hematite.

scattering domain in the [hkl] direction of crystal by Scherrer's equation. (110) and (111) reflection of goethite and (012) and (110) reflection of hamatite were used to calculate mean crystallite dimensions (MCD). The results are given in Table 2. Dimensions of goethite and hematite are less than 340Å. Nearly equal [110] and [111] dimensions of goethites of some reddish brown samples (D2-2, B29, E5) imply equal development of crystals in three directions and weak acicularity along c-direction. On the other hand, [110] dimensions of other samples including the yellowish brown are slightly larger than [110]

Table 2. Mean crystallite dimensions of goethite (G) and hematite(H) (in Å unit).

(hkl)	G_{110}	G_{111}	H_{012}	H_{110}
C13-3	200	284		
B29	199	207	200	290
B19	237	162		
G6	187	224	172	261
C17	148	165		
E5	340	319	215	291
D2-2	224	219	169	332
B25-2	117	163		
A12-2	177	230		
B28	227	281		

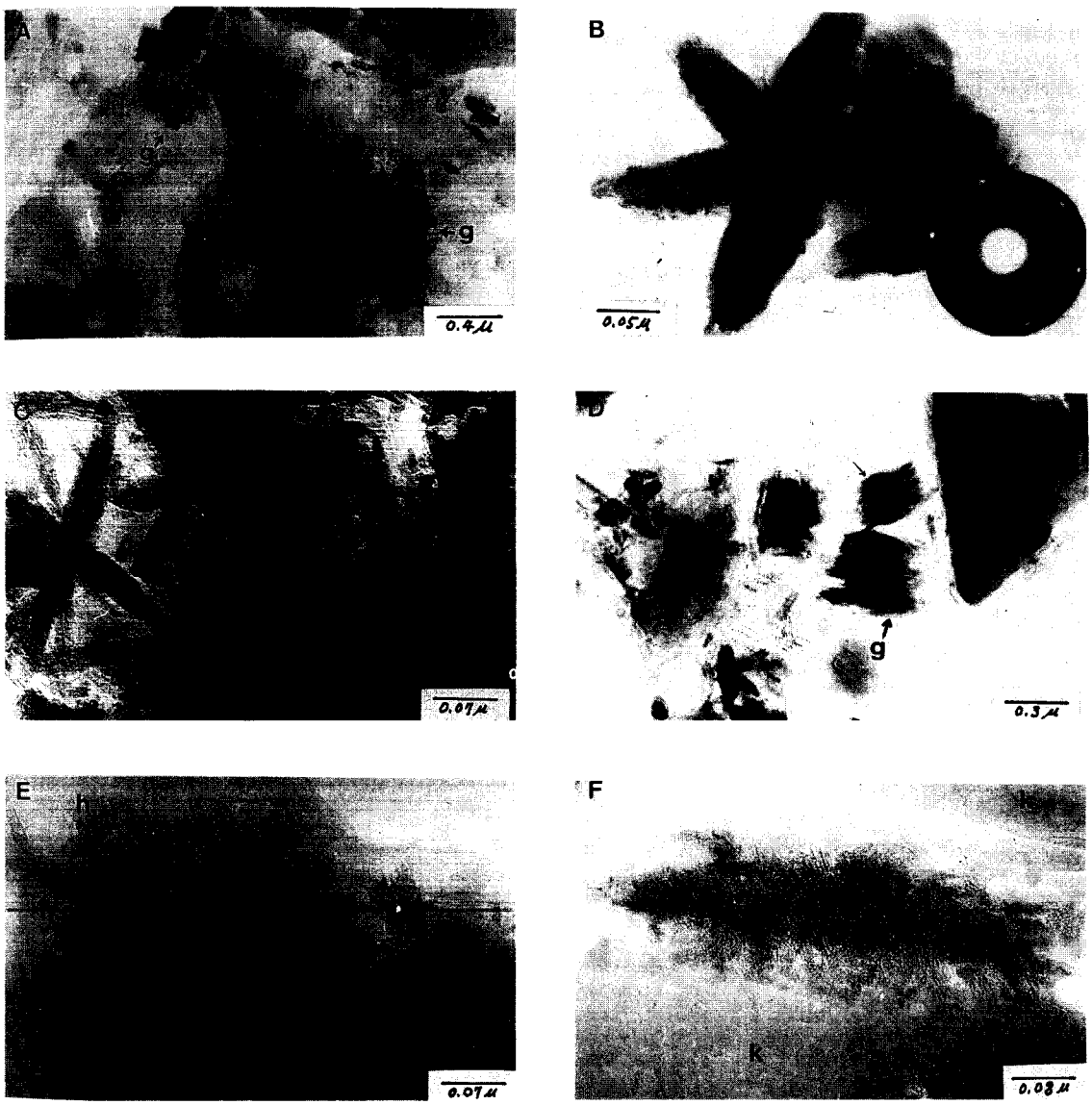

Fig. 3. Transmission electron micrographs of goethite concentrated by 5M NaOH method. (A) Star-shaped goethite(g) on the surface of vermiculite(v);(B) star-shaped goethite and its electron diffraction pattern showing six {040} spots;(C) lath and star-shaped goethite;(D) short bundles of goethite(g) and illite(i);(E) goethite(g) and halloysite(h) (epoxy-impregnated and ion-thinned specimen of reddish brown kaolin); (F) goethite(g) between the kaolinite(k) sheets altered from vermiculite (epoxy-impregnated and ion-thinned specimen of flake in the yellow spot of the reddish brown kaolin).

dimension. Such a difference in dimensions in two directions indicates that morphology of these goethites are more or less aciular in c-direction.

Hematites show larger [110] dimension than [012] implying that it has tabular morphology which is short in c-direction. Tabular character of hematite is also observed by the TEM observation.

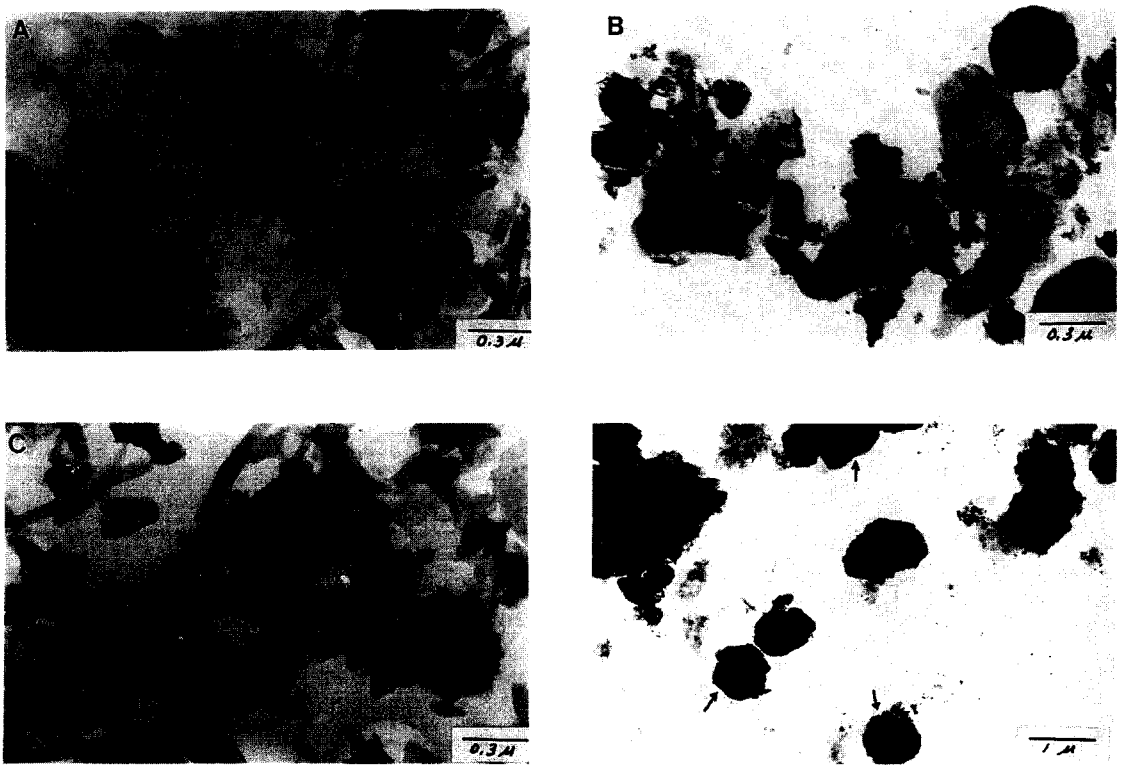

Fig. 4. Transmission electron micrographs of hematite. (A) Untreated reddish brown kaolin showing halloysite (long tube), hematite(spherical), and illite(plate); (B) hematite(dark spherical) and illite(plate) concentrated from reddish brown kaolin by 5M NaOH method; (C) untreated top red soil showing irregular shape hematite and halloysite; (D) concentrated hematite showing hexagonal outline(arrows) sampled in the red fissure.

Electron microscopy: TEM observation of the clay fraction of vermiculite samples shows that lath- and star-like goethite are attached on the vermiculite surface (Fig. 3a). Yellowish brown color of vermiculite is due to these fine goethite precipitates. Fig. 3b and 3c show well-developed star-shaped goethite crystal. The angles between laths are 60° and 120°. Electron diffraction pattern shows two sets of {040} spots diffracted from two laths crossing with 60°. Goet-hite consists of hexagonally close packed planes of oxygen atoms stacked along [100] and iron octahedra arranged in double rows which run along [001] (Eggleton et al., 1988). Therefore, the six direction growth of the goethite laths along the c-direction is possible on b-c plane, so that (021) twin planes are formed between two laths.

Goethite from the upper highly leached reddish brown kaolin has poor acicularity (Fig. 3b). They have short bundle or irreular shape. TEM micrograph of epoxy-impregnated and ion-thinned specimen (Fig. 3e) shows that poorly acicular goethites with halloysite tubes are precipitated in the open space. Vermiculite is altered to kaolinite in the upper reddish brown kaolin releasing iron. It is observed that goethite crystallizes between the kaolinite sheets (Fig. 3f).

Hematite shows some morphological variation like goethite. Electron micrographs of hematites in raw and 5M NaOH treated reddish brown kaolin are given, respectively, in Fig. 4a and 4b. There is no marked change in the

morphology of hematite before and after 5M NaOH treatment (Fig. 4a and 4b). Hematite from the top reddish brown soil shows irregular shape (Fig. 4c). These micrographs (Fig. 4a, 4b, and 4c) show that hematite in the upper reddish brown kaolin and soil has a spherical or irregular shape, and each grain appears to be aggregates rather than monocrystal. This fact supports that hematite is crystallized from ferrihydrite through the aggregation, arrange-ment, and dehydration (Fischer and Schwert-mann, 1975). Hematite from red fissure (Fig. 4d) shows more crystalline habit of a hexagonal outline.

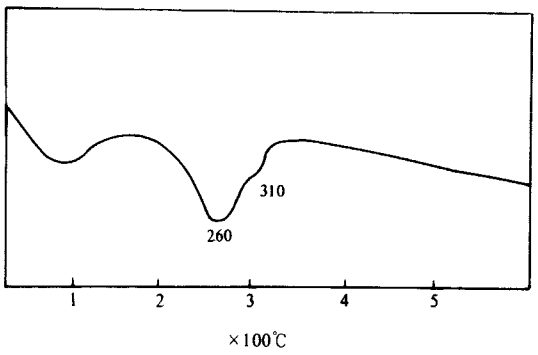

Fig. 5. Differential thermal curve of goethite.

Differential thermal analyses: Goethite shows two endothermic peaks at 260℃ and 310℃ (Fig. 5). It is known that two dehydroxylation peaks are due to two different crystallinities. Low crystallinity leads to a direct transformation into hematite but high crystallinity leads to a change in the unit cell size before forming hematite. Therefore, the endothermic peak of low crystalline goethite appears at low temperature, whereas that of high crystallinity at higher temperature (Schwertmann, 1984). Intensive endothermic peak at 260℃ implies that the crystallinity of Sancheong goethite is low.

Selective Dissolution

Selective dissolution result is tabulated in Table 3. High DCB extractable iron to total iron ratios (Fe_d/Fe_t) ranging from 0.55 to 0.90, imply that most of the iron of the clay fraction exists as DCB extractable discrete iron oxides.

Acid-oxalate extractable iron to total iron ratios (Fe_o/Fe_d) show a wide range of values. The yellow samples (B28, A12-2, B25-2) have very low values, whereas reddish brown or red samples slightly high values ranging from 0.07 to 0.74. The relative abundance of hematite to goethite is represented by the intensity ratio $I_{H(1D)}/(I_{H(1D)}+I_{G(1D)})$ where intensity is measured with peak height from background. The intensity ratio shows that yellow samples contain only goethite but reddish brown samples both goethite and hematite. Reddish brown samples of higher Fe_o/Fe_d always contain hematite. On the other hand, the yellow samples contain no hematite.

Table 3. Selectively extracted iron data for the clay fraction of the kaolin.

Sample	Fe_t[1]	Fe_d[2]	Fe_o[3]	Fe_d/Fe_t	Fe_o/Fe_d	color	$I_H/(I_H+I_G)$**
C13-3(U*)	1.98	1.09	0.81	0.55	0.74	Reddish brown	0.50
B29(S)	8.12	6.71	3.65	0.83	0.54	Reddish brown	0.60
B19(F)	1.88	1.43	0.22	0.76	0.15	Reddish brown	0.50
G6(U)	6.39	5.32	0.71	0.83	0.13	Reddish brown	0.52
C17(U)	3.39	3.01	0.32	0.89	0.11	Reddish brown	0.70
E5(U)	6.96	6.18	0.59	0.89	0.10	Red	0.79
D2-2(F)	12.63	7.98	0.56	0.63	0.07	Reddish brown	0.68
B25-2(L)	3.49	3.14	0.18	0.90	0.06	Yellow	0.00
A12-2(L)	2.36	1.69	0.06	0.72	0.04	Pinkish Yellow	0.00
B28(L)	4.54	3.76	0.09	0.83	0.02	Yellowish brown	0.00

1: Total iron, 2: Dithionite extractable iron, 3: Acid-oxalate extractable iron, * U, L, F, and S indicate respectively the samples from the Upper part of the kaolin, from the Lower part, Fissure, and Soil. ** I_H and I_G are the peak heights of Hematite (110) and Goethite (110) measured from background.

According to Campbell and Schwertmann (1984), there exists a linear relation between the strongest (110) peak of ferrihydrite and the oxalate soluble iron, and thus acid-oxalate extractable iron may simply indicate the presence of ferrihydrite. But the detection of acid-oxalate extractable iron does not directly evidence the presence of ferrihydrite because acid-oxalate treament extracts not only ferrihydrite but also poorly crystalline iron oxides. Ferrihydrite does not show any detectable peak in X-ray diffraction profile of mixture of several minerals due to its very low crystallinity. To disclose its diffraction pattern, differential X-ray diffraction method must be applied. It was attempted for sample B29 (raw and concentrate) to obtain differential X-ray diffraction pattern, but we failed to detect any notable diffraction pattern. This result suggests that acid-oxalate extractable iron of the kaolin was mostly extracted from poorly crystalline iron oxides. Transmission electron micrograph of hematite shows the possibility that hematite grain appears to be an aggregate of fine particles of ferrihydrite-hematite intergrade in the transformation. The acidoxalate extractable iron might also be extracted from these intermediate.

Formation of Goethite and Hematite

Fischer and Schwertmann (1975) reported, based on their synthetic study, that hematite is formed by the aggregation, rearrangement, and dehydration of structurally similar and highly disordered ferrihydrite but not by the direct precipitation from solution. In this study, ferrihydrite was not detected due to its very low content or abscence. It is interpreted that the abscence of ferrihydrite in hematitic soils can be explained by the fast transformation rate of ferrihydrite to hematite compared to that of the neoformation of ferrihydrite. Thus, it is not unreasonable that metastable ferrihydrite is not detected in the reddish brown kaolin. This consideration is supported by the low crystallinity of hematite observed in the TEM micrograph and relatively high Fe_o/Fe_d ratio of upper reddish brown kaolin. Ferrihydrite forms under condition of either rapid formation and/or retardation of goethite crystallization by impedent materials such as organics and silicates (Schwertmann, 1988b). Chukhrov (1981) suggested that at a late period of formation of weathering crust, bacterial activity decays the organic matter with evolving CO_2 during the rainy season. Then, Fe in goethite dissolves in favor of ferrobicarbonate. At dry season, Fe^{2+} is rapidly oxidized and forms ferrihydrite.

Goethite precipitates directly from solution or dissolving ferrihydrite, whereas hematite forms through the rearrangement of ferrihydrite and, thus, goethite and hematite formation is mutually competing reaction (Schwertmann, 1985). The factors that control the relative content between goethite and hematite are temperature, water activity, pH, organic matter, Al activity in the system, and release rate of Fe in the system (Schwertmann, 1988b). These factors vary with climate and profile depth.

The coexistence of hematite and goethite in the upper reddish brown kaolin reflects temperate climate in this area. Average annual rainfall in this area is 1354mm (Korea Meteorological Service, 1985) and most of it (1105mm) is confined on the season from April to September, especially in summer. Average annual air temperature is 12.7℃, but that from April to September is 20℃. Average annual relative humidity is 69%, and that during the rainy season is 72%. Therefore, the leaching reaction occurs mostly in this warm rainy season releasing iron by oxidation and dissolution.

In the upper reddish brown kaolin and soil, high amount of iron is supplied to the system from decomposing iron-rich silicates in the rainy season, and rapid precipitation of poorly crystalline iron oxides occurs. The presence of impeder such as organics and rich dissolved inorganics (mainly Si and Al species) from intensive leaching may hinder the crystallization of goethite. Instead, these conditions favor the formation of disordered ferrihydrite. Higher temperature in this season facilitates the formation of hematite through the aggregation and dehydration of ferrihydrite. On the contrary, high water activity in the rainy season and cool air temperature in winter are factors favoring the

formation of goethite. The presence of the hematite-goethite pair in the upper reddish brown kaolin indicates that climatic factors for the formation of two iron oxides overlap.

In the low white kaolin including yellow band and spot, release rate of iron and contents of organics and inorganics are low, whereas the water activity is high compared to that in the upper horizon. These conditions favor the precipitation of goethite instead of ferrihydrite formation.

The red color staining the upper kaolin is also found in vertical and network veinlet-like zone, or diffusion front in the yellow kaolin. The distribution of red color implies that solution containing iron species for precipitating iron oxides moved a few distance downward. The iron may be transported in the colloidal form or in the Fe^{2+} state from the upper reddish brown kaolin to the fissures precipitating iron oxides.

REFERENCES

Bailey, S. W. (1980) Summary of recommendation of AIPEA nomenclature committee. Clay Miner. 15, 85-93.

Brindley, G. W. (1980) Order-disorder in clay mineral structures. p. 125-195. In Crystal Structures of Clay Minerals and their X-Ray Identification (editors: G. W. Brindley and G. Goodman). The Mineralogical Society, London.

Caillière, S., Gatineau, L., and Hénin, S. (1960) Préparation à Basse température d'hématite alumineuse. C. R. Acad. Sci. 250, 3677-3679.

Campbell, A. S. and Schwertmann, U. (1984) Iron oxide mineralogy of placic horizons. J. Soil Sci. 35, 569-582.

Chukhrov, F. V. (1981) Lateritization Process, 11-14.

Eggleton, R. A., Schulze, D. G., and Stucki, J. W. (1988) Introduction to crystal structures of iron-containing minerals. p. 141-164. In Iron in Soils and Clay Minerals (editors: J. W. Stucki, B. A. Goodman, and U. Schwertmann). D. Reidel, Dordrecht.

Fischer, W. R. and Schwertmann, U. (1975) The formation of hematite from amorphous iron (III) hydroxide. Clays Clay Miner. 23, 33-37.

Jeong, G. Y. (1987) Mineralogy and genesis of kaolin from Sancheong area. M. S. Thesis, 81p, Seoul National University.

Kim, S. J., Jeong, G. Y., Lee, S. J., and Kwon, S. K. (1989) Mineralogy of kaolin from Hadong-Sancheong area, Korea. J. Miner. Soc. Korea 2, 11-17.

Klug, H. P. and Alexander, L. E. (1974) X-ray Diffraction Procedures for poycrystalline and Amorphous materials. 2nd edition. J. Wiley and Sons, New York.

Korea Meteological Service (1985) Climatic Summary of Korea.

Leake. B. E. (1978) Nomenclature of amphiboles. Canadian Miner. 16, 501-520.

Mehra, O. P. and Jackson, M. J. (1960) Iron oxide from soils and clays by a dithionite system buffered with sodium bicarbonate. Clays Clay Miner. 7, 317-327.

Norrish, K. and Taylor, R. M. (1961) The isomorphous replacement of iron by aluminum in soil goethite. J. Soil. Scil. 12, 294-306.

Schulze, D. G. (1981) Identification of soil iron oxide minerals by differential X-ray diffraction. Soil Sci. Soc. Am. J. 45, 437-440.

Schulze, D. G. (1984) The influence of aluminum on iron oxides, VIII. Unit cell dimension of Al-substituted goethites and estimation of Al from them. Clays Clay Miner. 32, 36-44.

Schwertmann, U. (1959) Die fraktionierte Extraktion der freien Eisenoxide in Büden, ihre mineralogischen Formen und ihre Entstehungsweisen. Z. Pflanzenernähr., Düng., Bodenk., 84, 194-204.

Schwertmann, U. (1984) The double dehydroxylation peak of goethite. Thermochimica Acta, 78, 39-46.

Schwertmann, U. (1985) The effect of pedogenic environments on iron oxide minerals. Advances in Soil Sciences, Vol. 1, 172-200.

Schwertmann, U. (1988a) Some properties of soils and synthetic iron oxides. P.203-250. In Iron in Soils and Clay Minerals (editors: J. W. Stucki, B. A. Goodman, and U. Schwertmann). D. Reidel, Dordrecht.

Schwertmann, U. (1988b) Occurrence and

formation of iron oxides in various pedoenvironmnts. p.267-308. In Iron In Soils and Clay Minerals (editors: J. W. Stucki, B. A. Goodman, and U. Schwertmann). D. Reidel, Dortrecht.

Schwertmann, U. and Taylor, R. M. (1977) Iron Oxides. p.145-175. In Minerals in Soil Environments (editors: J. B. Dixon and S. B. Weed). Soil Science Society of America.

Schwertmann, U. and Fechter (1984) The influence of aluminum on iron oxides. XI. Aluminum substituted maghemite in soils and its formation. Soil Sci. Soc. Am. J. 48, 1462-1463.

Schwertmann, U., Fitzpatrick, R. W., Taylor, R. M., and Lewis, D. G. (1979) The influence of aluminum on iron oxides. Part II. Preparation and properties of Al-substituted hematites. Clays Clay Miner. 27, 105-112,

Thiel, R. (1963). Zum System αFeOOH-αAlOOH. Z. Anorg. Allg. Chemie 326, 79-88.